

LETTER | MAY 23 2023

Linearized integrated microwave photonic circuit for filtering and phase shifting

Gaojian Liu ; Kaixuan Ye ; Okky Daulay ; Qinggui Tan; Hongxi Yu; David Marpaung  




APL Photonics 8, 051303 (2023)

<https://doi.org/10.1063/5.0148464>




CrossMark





yttrium iron garnet glassy carbon beamsplitters fused quartz additive manufacturing
zeolites III-IV semiconductors gallium lump copper nanoparticles organometallics
nano ribbons barium fluoride europium phosphors photonics infrared dyes
sapphire windows Nd:YAG epitaxial crystal growth ultra high purity materials transparent ceramics CIGS
spintronics raman substrates cerium oxide polishing powder cermet nanodispersions
silver nanoparticles perovskites surface functionalized nanoparticles Al Si P S Cl Ar MBE grade materials thin film
MOCVD beta-barium borate K Ca Sc Ti V Cr Mn Fe Co Ni Cu Zn Ga Ge As Se Br Kr OLED lighting solar energy
rare earth metals quantum dots Rb Sr Y Zr Nb Mo Tc Ru Rh Pd Ag Cd In Sn Sb Te I Xe sputtering targets fiber optics
osmium scintillation Ce:YAG Cs Ba La Hf Ta W Re Os Ir Pt Au Hg Tl Pb Bi Po At Rn h-BN deposition slugs
refractory metals laser crystals Fr Ra Ac Th Pa U Np Pu Am Cm Bk Cf Es Fm Md No Lr CVD precursors photovoltaics
anodic aluminum oxide niobate InAs wafers Ce Pr Nd Pm Sm Eu Gd Tb Dy Ho Er Tm Yb Lu metamaterials borosilicate glass
25th Anniversary logo MOFs AuNPs Th Pa U Np Pu Am Cm Bk Cf Es Fm Md No Lr YBCO superconductors InGaAs
ZnS CdTe The Next Generation of Material Science Catalogs indium tin oxide MgF2 rutile
perovskite crystals transparent ceramics diamond micropowder optical glass



Now Invent.™

www.americanelements.com

© 2001-2022, American Elements LLC, a U.S. Registered Trademark

Linearized integrated microwave photonic circuit for filtering and phase shifting

Cite as: APL Photon. 8, 051303 (2023); doi: 10.1063/5.0148464

Submitted: 1 March 2023 • Accepted: 8 May 2023 •

Published Online: 23 May 2023



View Online



Export Citation



CrossMark

Gaojian Liu,^{1,2}  Kaixuan Ye,¹  Okky Daulay,¹  Qinggui Tan,² Hongxi Yu,² and David Marpaung^{1,a)} 

AFFILIATIONS

¹Nonlinear Nanophotonics Group, MESA+ Institute of Nanotechnology, University of Twente, Enschede, The Netherlands

²China Academy of Space Technology (Xi'an), Xi'an, China

^{a)}Author to whom correspondence should be addressed: david.marpaung@utwente.nl

ABSTRACT

Photonic integration, advanced functionality, reconfigurability, and high radio frequency (RF) performance are key features in integrated microwave photonic systems that are still difficult to achieve simultaneously. In this work, we demonstrate an integrated microwave photonic circuit that can be reconfigured for two distinct RF functions, namely, a tunable notch filter and a phase shifter. We achieved >50 dB high-extinction notch filtering over 6–16 GHz and 2π continuously tunable phase shifting over 12–20 GHz frequencies. At the same time, we implemented an on-chip linearization technique to achieve a spurious-free dynamic range of more than $120 \text{ dB} \cdot \text{Hz}^{4/5}$ for both functions. Our work combines multi-functionality and linearization in one photonic integrated circuit and paves the way to reconfigurable RF photonic front-ends with very high performance.

© 2023 Author(s). All article content, except where otherwise noted, is licensed under a Creative Commons Attribution (CC BY) license (<http://creativecommons.org/licenses/by/4.0/>). <https://doi.org/10.1063/5.0148464>

INTRODUCTION

The development of cognitive and intelligent radio frequency (RF) systems calls for RF front-ends with multiple programmable functions.^{1,2} Microwave photonic (MWP) circuits with high bandwidth and flexible reconfigurability can play an important role in those modern RF systems.^{3–5} A number of approaches have been proposed to achieve programmable RF photonic circuits. Functionalities including filtering,^{6–10} phase shifting,^{11–15} and beamforming^{16–18} have been realized in application-specific photonic integrated circuits (PIC) that can achieve high performance. Another approach is to create general-purpose integrated MWP circuits that can be configured for a high number of functionalities. These circuits have been demonstrated in the form of waveguide mesh or micro-disk resonator arrays.^{19–22} Finally, cascaded MWP systems that can simultaneously perform notch filtering and phase shifting have also been demonstrated in Refs. 23 and 24.

To be relevant for real-world applications, MWP circuits need to be more than just programmable. Sufficient RF performance, such as a low noise figure and high spurious-free dynamic range (SFDR), is also required so that they can be placed at the beginning

of the RF front-end chain, where the broad bandwidth is most needed.

However, to date, most demonstrated integrated MWP systems are plagued by poor SFDR.^{6,10,25,26} There is an opportunity to circumvent this problem by implementing linearization techniques.^{27–30} However, only very recently can RF photonic functionality and linearization be simultaneously achieved in the same system, for example, in fiber-based phase shifters³¹ or in a chip-based programmable filter.³² Extending this concept to the multi-functional circuit will be important for the MWP field.

In this work, we present a reconfigurable integrated MWP circuit that can perform two distinct functionalities, i.e., a tunable notch filter and a 2π -range phase shifter, while maintaining an ultra-high SFDR. The tunable notch filter function can achieve a rejection of more than 50 dB with a 3-dB bandwidth of 315 MHz from 6 to 16 GHz. In the meantime, the tunable phase shifter function can realize 2π continuous tuning range from 12 to 20 GHz. Moreover, both functions can provide an SFDR larger than $120 \text{ dB} \cdot \text{Hz}^{4/5}$. This work shows the important first step toward high-performance integrated MWP subsystems with a large number of RF functions.

RESULTS

Reconfigurable integrated MWP circuit

The concept of our reconfigurable integrated MWP circuit is illustrated in Fig. 1. It can serve as a notch filter or a phase

shifter with different configurations. By manipulating the phases and amplitudes of multi-order optical sidebands independently, both functionalities can also exhibit an ultrahigh dynamic range.

The multi-functional integrated MWP circuit is fabricated with the Si₃N₄ TriPleX process.^{33,34} Figure 1(a) shows the micrograph of

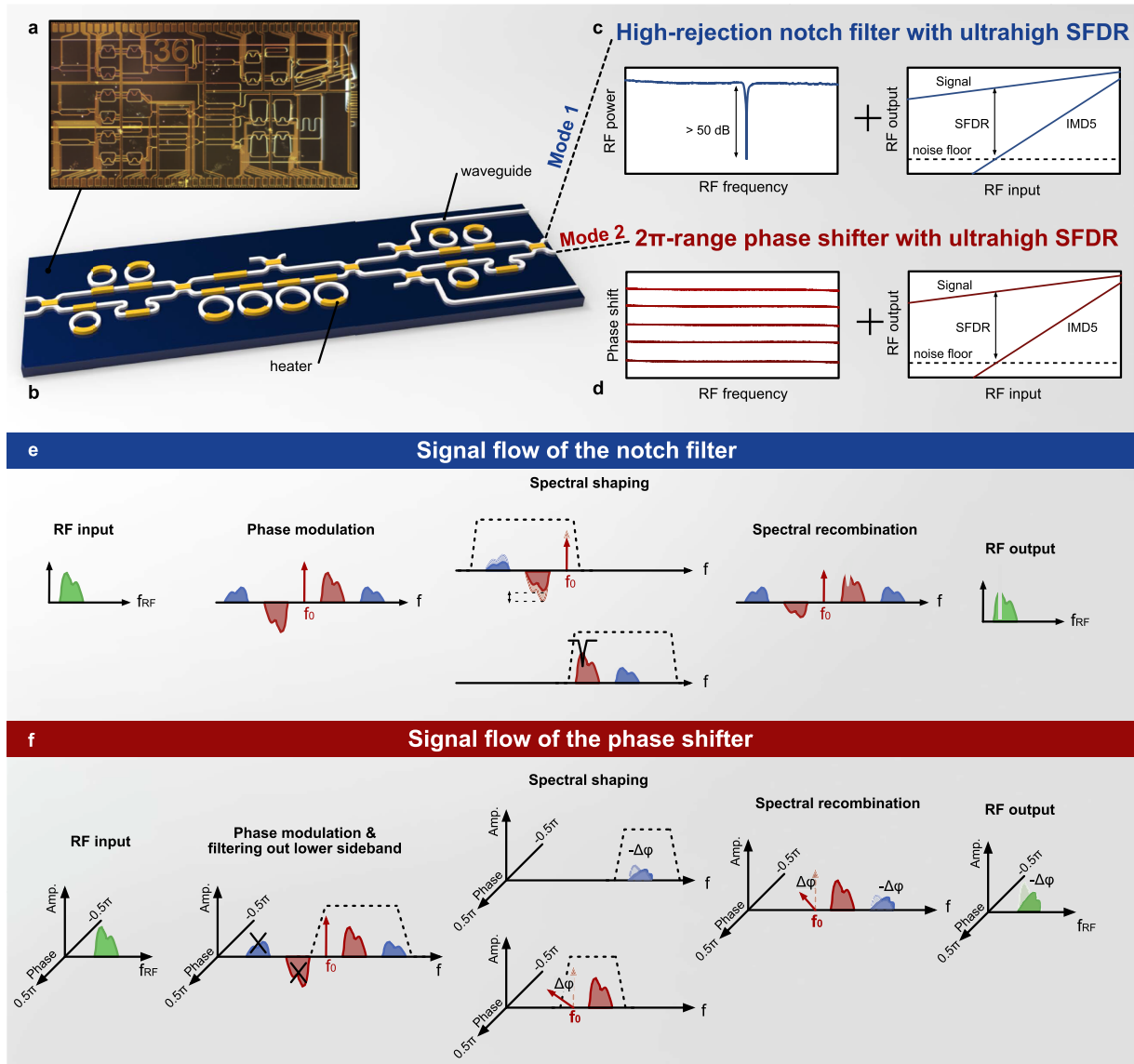


FIG. 1. Concept of the reconfigurable integrated MWP circuit with enhanced dynamic range. (a) The micrograph of the fabricated chip. (b) Schematic of the reconfigurable integrated MWP circuit. (c) and (d) The illustration of the achieved functionalities, i.e., the high-rejection notch filter and the 2π -range phase shifter. (e) For the linearized notch filter, we first spatially separate the phase-modulated light into two paths on the chip. Then, in one path, the carrier and lower sidebands are attenuated to create asymmetric double sidebands. Meanwhile, the first-order upper sideband in the other path is processed with a shallow over-coupled ring to have equal amplitude and anti-phase at the notch frequency. The two paths are then recombined, and a high rejection MWP notch filter is created based on the RF interference. (f) For the linearized phase shifter, we first filter out the lower sidebands of the phase-modulated light with an off-chip bandpass filter. Then, the on-chip deinterleaver separates the second-order upper sideband from the carrier and the first-order upper sideband. After that, two over-coupled rings are applied at the carrier to introduce phase shift. In the meantime, an opposite phase shift is applied to the second-order sideband with the optical phase shifter in the other path. Signals from both paths are then recombined, and a linearized phase shifter is created when all signals are converted back into the RF domain.

14 December 2023 13:32:06

the chip. It consists of two spectral deinterleavers, a tunable attenuator, an optical phase shifter, and an array of all-pass ring resonators, as illustrated in Fig. 1(b). The spectral deinterleavers are implemented with an asymmetric Mach–Zehnder interferometer (aMZI) loaded with 3 ring resonators,³⁵ exhibiting flat-top complementary filter response with a free spectral range (FSR) of 160 GHz.²⁹ The array of all-pass ring resonators (FSR of 50 GHz) between the two deinterleavers has a tunable coupling ratio and round trip phase that can be controlled via thermo-optic tuning. By applying different voltages to the microheaters, this chip can be configured as a notch filter or a phase shifter while maintaining an ultrahigh SFDR, as indicated in Figs. 1(c) and 1(d).

The signal processing of both functionalities, as shown in Figs. 1(e) and 1(f), follows a similar procedure. First, the deinterleaver separates the input optical spectrum into two paths. The attenuator and phase shifter in the upper path change the relative phase and amplitude between the two paths for wideband spectrum shaping. In the lower path, an array of all-pass ring resonators performs narrowband phase and amplitude tailoring with high precision. The signals in the two paths are then recombined and directly coupled out of the chip or coupled into the second deinterleaver for further processing. By tailoring the amplitudes and phases of the optical carrier and multi-order sidebands in such a manner, the third-order intermodulation distortion (IMD3) from beating products between different optical sidebands can destructively interfere with each other, leading to an ultrahigh dynamic range.

High-rejection notch filter with ultrahigh SFDR

We first configure this multi-functional MWP circuit into a high-rejection notch filter with enhanced SFDR. A phase-modulated optical signal is sent to the programmable photonic chip for spectral shaping. Because of the nonlinearity of the phase modulator, the

modulated optical signal consists of multi-order sidebands, among which the \pm first-order sidebands have a π phase difference. We use the spectral deinterleaver to first separate the optical carrier and lower sidebands from the upper sidebands. Then, the lower sidebands and optical carrier are attenuated to generate the asymmetric double sideband (aDSB) spectrum while simultaneously satisfying the linearization condition.³² Meanwhile, an under-coupled ring resonator imposes a shallow notch at the upper sideband to meet equal amplitude and anti-phase conditions at the notch frequency. After that, the signal is recombined, and a high rejection MWP notch filter based on RF interference is created.³⁶ Because of the destructive interference between different IMD3 components, the linearity of the notch filter can be significantly improved (see the supplementary material for more experimental details).

The performance of the linearized MWP notch filter is shown in Fig. 2. To highlight the advantages of our filter, we compared it with a standard single sideband (SSB) modulated MWP notch filter using the same ring response without linearization. Our demonstrated notch filter has a notch rejection of 52 dB and a 3-dB bandwidth of 315 MHz (at the center frequency of 12 GHz), as shown in Fig. 2(a). We also performed the two-tone test to evaluate the linearity of the demonstrated notch filter. The results shown in Fig. 2(b) exhibit an IMD3 suppression of 28.7 dB when the two-tone RF frequency is at 9 GHz with a spacing of 10 MHz. The large suppression of the IMD3 makes the fifth-order nonlinearity dominate, leading to SFDR improvement from $103.8 \text{ dB} \cdot \text{Hz}^{2/3}$ to $123.6 \text{ dB} \cdot \text{Hz}^{4/5}$ with a noise floor of -164.5 dBm/Hz , as observed in Fig. 2(c). Moreover, the filter maintains high rejection and a large SFDR during the tuning of the notch frequency, as shown in Fig. 2(d). The filter shows a link gain of -26.3 dB and a noise figure (NF) of 35.8 dB . This moderate gain and NF are because of the partially destructive interference between two first-order sidebands (see the supplementary material for extended measurement results).

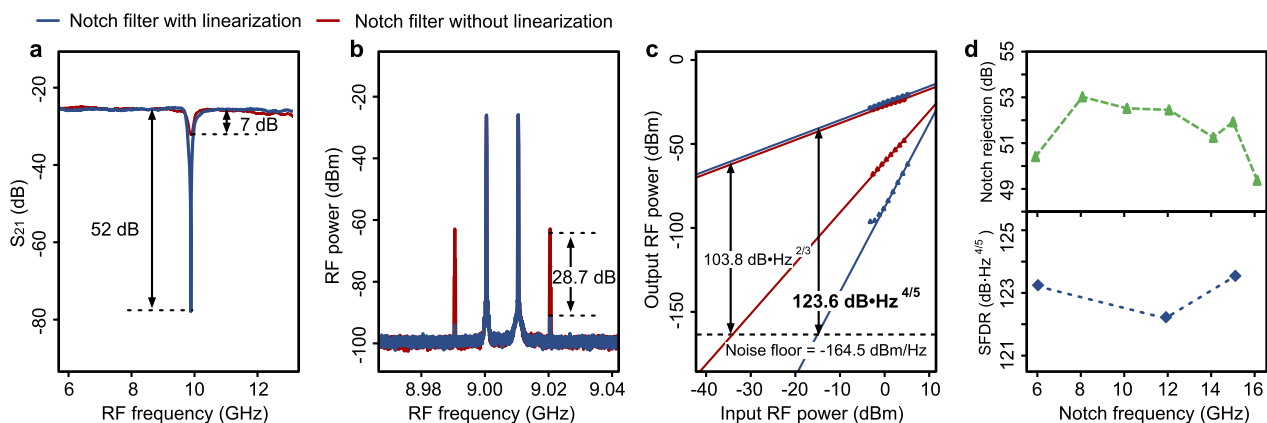


FIG. 2. High-rejection notch filter with an ultrahigh dynamic range. (a) Measured linearized RF notch response with a rejection of 52 dB compared with the benchmarked single-sideband (SSB) RF notch filter. (b) The measured two-tone RF spectra at the output of the photodetector for the linearized RF notch filter (blue) and single-sideband (SSB) RF notch filter without linearization (red) with a 28.7 dB reduction of IMD3 power. (c) The measured spurious-free dynamic range (SFDR) of the proposed linearized notch filter and SSB notch filter without linearization at an RF frequency of 9 GHz. The proposed linearized filter has a record-high SFDR of $123.6 \text{ dB} \cdot \text{Hz}^{4/5}$. (d) The measured rejection of the linearized notch filter and the SFDR at 9 GHz with the tuning of the notch frequency.

2π -range phase shifter with ultrahigh SFDR

The chip can also be reconfigured as a 2π -range tunable phase shifter while maintaining the ultrahigh dynamic range. To realize the phase shifting function, we first use an external bandpass filter (BPF) to remove the lower sideband of the phase-modulated optical signal. We also attenuate the optical carrier with the BPF by positioning the optical carrier at the transition band for the purpose of linearization. The preprocessed single-sideband (SSB) optical signal is then coupled into the chip. We separate the optical carrier and the +first-order sideband from the +second-order sideband with the spectral deinterleaver. By applying two over-coupled ring resonators at the optical carrier, the 2π -range phase shift is introduced with negligible amplitude variation. The optical phase shift is then converted to the RF phase shift when the optical carrier beats with the +first-order sideband at the photodetector (see the supplementary material for the experimental setup). To suppress the IMD3 and improve the linearity of the phase shifter, both amplitude and phase conditions between the optical carrier and the +second-order sideband need to be satisfied (see the supplementary material for the linearization method). On the one hand, we adjust the power ratio between the optical carrier and +second-order sideband by controlling the passband location of the external BPF and the coupling coefficients of the ring resonators. On the other hand, we tune the phase of the +second-order sideband with an optical phase shifter to satisfy the phase condition, while the MWP phase shifter tunes over the 2π range.

The performance of the demonstrated phase shifter is presented in Fig. 3. We can realize continuous phase tuning over the 2π range by adjusting the resonance frequencies of the two over-coupled rings. Because of the relatively flat stopband response of the two cascaded ring resonators, the amplitude fluctuation of the phase shifter is less than 1 dB over the whole 2π range, as shown in Fig. 3(a). To evaluate the linearity of the demonstrated phase shifter, we also conducted a two-tone test and compared the results with a

phase shifter without linearization for the same phase shift (0.6π in this case). As shown in Fig. 3(b), the linearized phase shifter exhibits an improved fundamental to IMD3 ratio of 20 dB. As a result, the SFDR of the phase shifter increases from $105.2\text{ dB} \cdot \text{Hz}^{2/3}$ to $121.2\text{ dB} \cdot \text{Hz}^{4/5}$, which is shown in Fig. 3(c). The noise floor of both phase shifters is -146.8 dBm/Hz . The phase shifter exhibits a link gain of -5.8 dB and an NF of 33 dB. The NF of the proposed phase shifter is mainly deteriorated by the phase noise-to-intensity noise conversion of the laser when the optical carrier is attenuated by the external BPF.

DISCUSSION AND CONCLUSION

In this work, we demonstrated a multi-functional integrated MWP circuit that can be reconfigured between a high-rejection notch filter and a 2π -range phase shifter. By vectorially manipulating the multi-order optical sidebands, an ultrahigh dynamic range over $120\text{ dB} \cdot \text{Hz}^{4/5}$ is achieved in both functions. Table I compares this work with the state-of-the-art MWP circuits. While application-specific MWP circuits already show a wide operating frequency band, RF performances, including link gain, NF, and SFDR, are still relatively poor or not available in most demonstrations. Very recently, reconfigurable MWP circuits with relatively high RF performance have been realized in Refs. 10, 32, and 40; however, only the filter functions are demonstrated.

On the contrary, we demonstrated two distinct functionalities, namely, filter and phase shifting, while maintaining high linearity in this work. The array of microring resonators and two spectral deinterleavers could potentially unlock even more functionalities, for example, true time delay. Moreover, the possibility to realize multiple different functions in one circuit also opens the path to the cascaded integrated MWP system, which would be a major leap toward integrated RF photonic front-ends that can be directly applied in real RF environments.

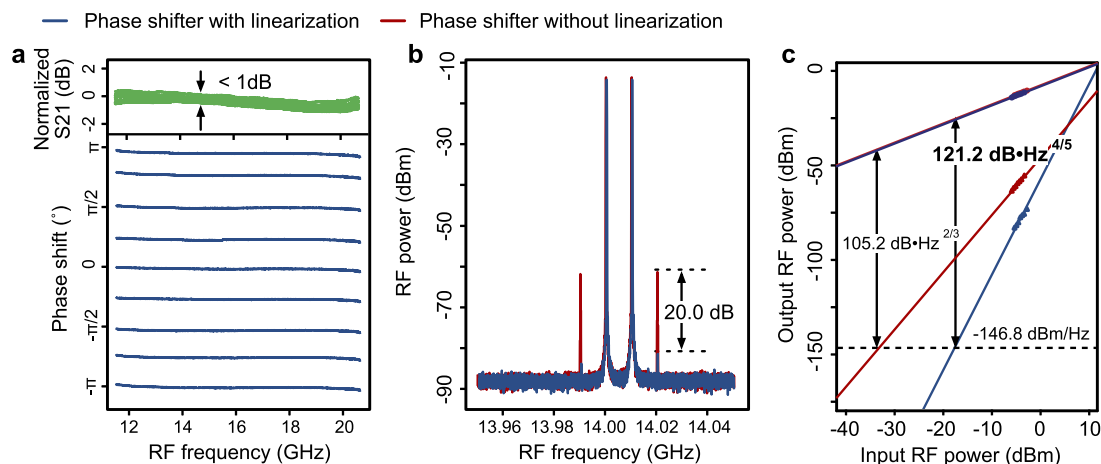


FIG. 3. 2π -range tunable phase shifter with ultrahigh dynamic range. (a) The phase tuning of the proposed phase shifter over 2π . The phase response is flat in the range of 12–20 GHz. (b) The measured two-tone RF spectra at the output of the photodetector for the linearized RF phase shifter (blue) and bench-marked RF phase shifter without linearization (red) with a 20.0 dB improvement in the fundamental to IMD3 ratio. (c) The measured spurious-free dynamic range (SFDR) of the proposed linearized phase shifter and the bench-marked phase shifter without linearization at an RF frequency of 14 GHz. The proposed phase shifter exhibits a record-high SFDR of $121.2\text{ dB} \cdot \text{Hz}^{4/5}$.

TABLE I. Performance comparison with the state-of-the-art MWP circuits.

Year and reference	Functionalities	Platform	Frequency band (GHz)	Link gain (dB)	NF (dB)	SFDR (dB · Hz ^{2/3})
2022 ³⁷	Notch filter (notch)	SOI	8–14	–3.6	52.5	93.6
2023 ³⁸	Notch	PhC ^a	1–40	N/A	N/A	N/A
2022 ²⁶	Bandpass filter (BPF)	SOI	5.2–35.8	8.97	33	88.93
2020 ¹⁴	Phase shifter (PS)	Si ₃ N ₄	12–23	N/A	N/A	N/A
2021 ³¹	PS	Fiber	12–22	N/A	N/A	125.7
2022 ³⁹	PS	SOI	20–40	N/A	N/A	N/A
2021 ¹⁰	BPF/notch	Hybrid ^b	3–21/3–25	–28.2	51.2	99.7
2022 ³²	BPF/notch	Si ₃ N ₄	4–20/6–18	10/–26	15/35	116/123
2023 ^{40,c}	Allpass filter (APF)/BPF/notch	SOI	20–43.5	9	23	112
This work	Notch/PS	Si ₃ N ₄	6–18/12–20	–26.3/–5.8	35.8/33	123.6/121.2

^aPhC: Photonic crystal.

^bHybrid: InP for the active devices and SOI for the passive devices.

^cOnly the measurement results without using the RF pre-amplifier are listed.

Currently, the reconfigurable MWP circuit in this work exhibits relatively low link gain and a high noise figure. In principle, the link gain can be improved by increasing the optical power of a high power-handling modulator. The strategy for noise figure reduction, on the other hand, is more intricate. The use of the phase modulator in our experiments prevents NF reduction techniques such as low-biasing a Mach-Zehnder intensity modulator³² from being employed. Emulation of such a technique using carrier processing by a ring resonator has been previously considered,⁸ but the power builds up in the high-Q ring used for carrier processing, preventing effective NF reduction. We believe that achieving simultaneous high link gain and low NF together with the features demonstrated in this work will require an entirely new topology potentially using a more complex interferometric modulator (for example, dual-drive or dual-parallel MZM) with on-chip linearization. Several recent studies have shown encouraging results in this direction.^{30,41}

Another direction to improve our reconfigurable MWP circuit is to integrate active devices with passive devices on a single chip.¹⁰ Currently, our system still utilizes discrete components for the laser, modulator, amplifier, and photodetector. However, encouraging progress has been made in the development of the low-RIN lasers in the hybrid silicon nitride-InP platform⁴² as well as the high-gain erbium-doped amplifiers in silicon nitride waveguides.⁴³ Although the integration of all these advancements will require considerable effort and dedicated designs, it will ultimately lead to the creation of an all-integrated, multi-functional MWP circuit with superior RF performance.

SUPPLEMENTARY MATERIAL

See the supplementary material for the setup and experimental details.

ACKNOWLEDGMENTS

The authors acknowledge funding from the European Research Council Consolidator Grant (101043229 TRIFFIC) and the

Nederlandse Organisatie voor Wetenschappelijk Onderzoek (NWO) Vidi (15702) and Start Up (740.018.021).

AUTHOR DECLARATIONS

Conflict of Interest

The authors have no conflicts to disclose.

Author Contributions

Gaojian Liu and Kaixuan Ye contributed equally to this work. D.M. and G.L. developed the concept and proposed the physical system. O.D. designed the photonic circuits. G.L. and K.Y. developed and performed numerical simulations. G.L. and K.Y. performed the experiments with input from O.D. D.M., G.L., and K.Y. wrote the article with input from Q.T. and H.Y. D.M. led and supervised the entire project.

Gaojian Liu: Conceptualization (equal); Data curation (equal); Formal analysis (equal); Investigation (equal); Methodology (equal); Validation (equal); Visualization (equal); Writing – original draft (equal); Writing – review & editing (equal). **Kaixuan Ye:** Data curation (equal); Formal analysis (equal); Investigation (equal); Methodology (equal); Validation (equal); Visualization (equal); Writing – original draft (equal); Writing – review & editing (equal). **Okky Daulay:** Data curation (equal); Formal analysis (equal); Investigation (equal); Methodology (equal); Validation (equal). **Qinggui Tan:** Formal analysis (equal); Investigation (equal); Methodology (equal); Writing – review & editing (equal). **Hongxi Yu:** Formal analysis (equal); Investigation (equal); Methodology (equal); Writing – review & editing (equal). **David Marpaung:** Conceptualization (equal); Data curation (equal); Formal analysis (equal); Funding acquisition (equal); Investigation (equal); Methodology (equal); Project administration (equal); Supervision (equal); Validation (equal); Visualization (equal); Writing – original draft (equal); Writing – review & editing (equal).

DATA AVAILABILITY

The data that support the findings of this study are available from the corresponding authors upon reasonable request.

REFERENCES

- ¹C. Baylis, M. Fellows, L. Cohen, and R. J. Marks II, "Solving the spectrum crisis: Intelligent, reconfigurable microwave transmitter amplifiers for cognitive radar," *IEEE Microwave Mag.* **15**(5), 94–107 (2014).
- ²H. Islam, S. Das, T. Bose, and T. Ali, "Diode based reconfigurable microwave filters for cognitive radio applications: A review," *IEEE Access* **8**, 185429–185444 (2020).
- ³J. Capmany and D. Novak, "Microwave photonics combines two worlds," *Nat. Photonics* **1**(6), 319 (2007).
- ⁴D. Marpaung, J. Yao, and J. Capmany, "Integrated microwave photonics," *Nat. Photonics* **13**(2), 80–90 (2019).
- ⁵D. Zhu and S. Pan, "Broadband cognitive radio enabled by photonics," *J. Lightwave Technol.* **38**(12), 3076–3088 (2020).
- ⁶J. S. Fandiño, P. Muñoz, D. Doménech, and J. Capmany, "A monolithic integrated photonic microwave filter," *Nat. Photonics* **11**(2), 124–129 (2017).
- ⁷Y. Liu, A. Choudhary, D. Marpaung, and B. J. Eggleton, "Integrated microwave photonic filters," *Adv. Opt. Photonics* **12**(2), 485–555 (2020).
- ⁸O. Daulay, R. Botter, and D. Marpaung, "On-chip programmable microwave photonic filter with an integrated optical carrier processor," *OSA Continuum* **3**(8), 2166–2174 (2020).
- ⁹Y. Chen, Z. Fan, Y. Lin, D. Jiang, X. Li, and Q. Qiu, "A multiband microwave photonic filter based on a strongly coupled microring resonator with adjustable bandwidth," *IEEE Photonics J.* **15**(1), 5500206 (2023).
- ¹⁰Y. Tao, H. Shu, X. Wang, M. Jin, Z. Tao, F. Yang, J. Shi, and J. Qin, "Hybrid-integrated high-performance microwave photonic filter with switchable response," *Photonics Res.* **9**(8), 1569–1580 (2021).
- ¹¹S. X. Chew, S. Song, L. Li, L. Nguyen, and X. Yi, "Inline microring resonator based microwave photonic phase shifter with self-mitigation of RF power variations," *J. Lightwave Technol.* **40**(2), 442–451 (2022).
- ¹²C. Porzi, G. Serafino, M. Sans, F. Falconi, V. Soriano, S. Pinna, J. E. Mitchell, M. Romagnoli, A. Bogoni, and P. Ghelfi, "Photonic integrated microwave phase shifter up to the mm-wave band with fast response time in silicon-on-insulator technology," *J. Lightwave Technol.* **36**(19), 4494–4500 (2018).
- ¹³L. McKay, M. Merklein, A. C. Bedoya, A. Choudhary, M. Jenkins, C. Middleton, A. Cramer, J. Devenport, A. Klee, R. DeSalvo *et al.*, "Brillouin-based phase shifter in a silicon waveguide," *Optica* **6**(7), 907–913 (2019).
- ¹⁴D. Lin, X. Xu, P. Zheng, G. Hu, B. Yun, and Y. Cui, "A high-performance microwave photonic phase shifter based on cascaded silicon nitride microrings," *IEEE Photonics Technol. Lett.* **32**(19), 1265–1268 (2020).
- ¹⁵S. X. Chew, D. Huang, L. Li, S. Song, M. A. Tran, X. Yi, and J. E. Bowers, "Integrated microwave photonic phase shifter with full tunable phase shifting range (> 360°) and RF power equalization," *Opt. Express* **27**(10), 14798–14808 (2019).
- ¹⁶C. Zhu, L. Lu, W. Shan, W. Xu, G. Zhou, L. Zhou, and J. Chen, "Silicon integrated microwave photonic beamformer," *Optica* **7**(9), 1162–1170 (2020).
- ¹⁷P. M.-C. Romero, D. P. López, D. P. Galacho, T. Ho, D. Wessel, and J. C. Francoy, "High-precision broadband silicon photonics beamformer," in *2022 IEEE International Topical Meeting on Microwave Photonics (MWP)* (IEEE, 2022), pp. 1–4.
- ¹⁸D. Lin, S. Shi, P. Liu, W. Cheng, M. Lu, T. Lin, G. Hu, B. Yun, and Y. Cui, "Low loss silicon nitride 1 × 4 microwave photonic beamforming chip," *Opt. Express* **30**(17), 30672–30683 (2022).
- ¹⁹L. Zhuang, C. G. H. Roeloffzen, M. Hoekman, K.-J. Boller, and A. J. Lowery, "Programmable photonic signal processor chip for radiofrequency applications," *Optica* **2**(10), 854–859 (2015).
- ²⁰D. Pérez, I. Gasulla, L. Crudgington, D. J. Thomson, A. Z. Khokhar, K. Li, W. Cao, G. Z. Mashanovich, and J. Capmany, "Multipurpose silicon photonics signal processor core," *Nat. Commun.* **8**(1), 636 (2017).
- ²¹W. Bogaerts, D. Pérez, J. Capmany, D. A. B. Miller, J. Poon, D. Englund, F. Morichetti, and A. Melloni, "Programmable photonic circuits," *Nature* **586**(7828), 207–216 (2020).
- ²²W. Zhang and J. Yao, "Photonic integrated field-programmable disk array signal processor," *Nat. Commun.* **11**(1), 406 (2020).
- ²³S. X. Chew, L. Nguyen, X. Yi, S. Song, L. Li, P. Bian, and R. Minasian, "Distributed optical signal processing for microwave photonics subsystems," *Opt. Express* **24**(5), 4730–4739 (2016).
- ²⁴X. Xue, X. Zheng, H. Zhang, and B. Zhou, "All-optical microwave bandpass filter and phase shifter using a broadband optical source and an optical phase modulator," *Opt. Lett.* **37**(10), 1661–1663 (2012).
- ²⁵Y. Yao, Y. Zhao, J. Dong, and X. Zhang, "Silicon integrated frequency-tunable microwave photonic bandpass filter," *IET Optoelectron.* (published online) (2022).
- ²⁶Y. Liu, Y. Chen, L. Wang, Y. Yu, Y. Yu, and X. Zhang, "Tunable and reconfigurable microwave photonic bandpass filter based on cascaded silicon microring resonators," *J. Lightwave Technol.* **40**(14), 4655–4662 (2022).
- ²⁷R. Wu, T. Jiang, S. Yu, J. Shang, and W. Gu, "Multi-order nonlinear distortions analysis and suppression in phase modulation microwave photonics link," *J. Lightwave Technol.* **37**(24), 5973–5981 (2019).
- ²⁸W. Wang, Y. Bai, S. Fu, X. Su, Y. Gu, H. Chi, M. Zhao, and X. Han, "High linearity microwave photonic up-conversion system based on parallel dual-drive Mach-Zehnder modulators," *Photonics* **9**(4), 236 (2022).
- ²⁹G. Liu, O. Daulay, Y. Klaver, R. Botter, Q. Tan, H. Yu, M. Hoekman, E. J. Klein, and D. Marpaung, "Integrated microwave photonic spectral shaping for linearization and spurious-free dynamic range enhancement," *J. Lightwave Technol.* **39**, 7551 (2021).
- ³⁰L. Torrijos-Moran, C. Catala-Lahoz, D. Perez-Lopez, L. Xu, W. Tianxiang, and D. Perez-Galacho, "Linearization of a dual-parallel Mach-Zehnder modulator using optical carrier band processing," *J. Lightwave Technol.* **41**, 2969 (2023).
- ³¹Y. Bai, X. Song, Z. Su, Z. Zheng, H. Zhang, X. Gao, and S. Huang, "Large dynamic range microwave photonic phase shifter based on multi-order sidebands optical spectrum vector process technique," in *2021 Optical Fiber Communications Conference and Exhibition (OFC)* (IEEE, 2021), pp. 1–3.
- ³²O. Daulay, G. Liu, K. Ye, R. Botter, Y. Klaver, Q. Tan, H. Yu, M. Hoekman, E. Klein, C. Roeloffzen *et al.*, "Ultra-high dynamic range and low noise figure programmable integrated microwave photonic filter," *Nat. Commun.* **13**(1), 7798 (2022).
- ³³C. G. H. Roeloffzen, M. Hoekman, E. J. Klein, L. S. Wevers, R. B. Timens, D. Marchenko, D. Geskus, R. Dekker, A. Alippi, R. Grootjans *et al.*, "Low-loss Si₃N₄ triplex optical waveguides: Technology and applications overview," *IEEE J. Sel. Top. Quantum Electron.* **24**(4), 1–21 (2018).
- ³⁴K. Wörhoff, R. G. Heideman, A. Leinse, and M. Hoekman, "Triplex: A versatile dielectric photonic platform," *Adv. Opt. Technol.* **4**(2), 189–207 (2015).
- ³⁵L.-W. Luo, S. Ibrahim, A. Nitkowski, Z. Ding, C. B. Poitras, S. J. Ben Yoo, and M. Lipson, "High bandwidth on-chip silicon photonic interleaver," *Opt. Express* **18**(22), 23079–23087 (2010).
- ³⁶D. Marpaung, B. Morrison, R. Pant, C. Roeloffzen, A. Leinse, M. Hoekman, R. Heideman, and B. J. Eggleton, "Si₃N₄ ring resonator-based microwave photonic notch filter with an ultrahigh peak rejection," *Opt. Express* **21**(20), 23286–23294 (2013).
- ³⁷S. Gertler, N. T. Otterstrom, M. Gehl, A. L. Starbuck, C. M. Dallo, A. T. Pomerene, D. C. Trotter, A. L. Lentine, and P. T. Rakich, "Narrowband microwave-photonic notch filters using Brillouin-based signal transduction in silicon," *Nat. Commun.* **13**(1), 1947 (2022).
- ³⁸L. Liu, M. Ye, Z. Yu, and W. Xue, "Notch microwave photonic filter with narrow bandwidth and ultra-high all-optical tuning efficiency based on a silicon nanobeam cavity," *J. Lightwave Technol.* (published online) (2023).
- ³⁹S. X. Chew, X. Yi, and L. Nguyen, "Microwave photonic phase shifter based on the integration of ITO-enabled microheaters," in *2022 IEEE International Topical Meeting on Microwave Photonics, MWP 2022 - Proceedings, 2022*.

⁴⁰R. Rady, C. Madsen, S. Palermo, and K. Entesari, “A 20-43.5-GHz wideband tunable silicon photonic receiver front-end for mm-wave channel selection/jammer rejection,” *J. Lightwave Technol.* **41**, 1309–1324 (2023).

⁴¹H. Feng, K. Zhang, W. Sun, Y. Ren, Y. Zhang, W. Zhang, and C. Wang, “Ultra-high-linearity integrated lithium niobate electro-optic modulators,” *Photonics Res.* **10**, 2366 (2022).

⁴²Y. Fan, A. van Rees, P. J. M. van der Slot, J. Mak, R. M. Oldenbeuving, M. Hoekman, D. Geskus, C. G. H. Roeloffzen, and K.-J. Boller, “Hybrid integrated InP-Si₃N₄ diode laser with a 40-Hz intrinsic linewidth,” *Opt. Express* **28**, 21713–21728 (2020).

⁴³Y. Liu, Z. Qiu, X. Ji, A. Lukashchuk, J. He, J. Riemensberger, M. Hafermann, R. N. Wang, J. Liu, C. Ronning, and T. J. Kippenberg, “A photonic integrated circuit-based erbium-doped amplifier,” *Science* **376**(6599), 1309–1313 (2022).